Molecular and supramolecular chemistry of mono- and di-selenium analogues of metal dithiocarbamates

See Mun Lee,[a] Peter J. Heard[b] and Edward R. T. Tiekink[a,*]

[a] Research Centre for Crystalline Materials, School of Science and Technology, Sunway University, No. 5 Jalan Universiti, 47500 Bandar Sunway, Selangor Darul Ehsan, Malaysia

[b] Office of the Provost, Sunway University, No. 5 Jalan Universiti, 47500 Bandar Sunway, Selangor Darul Ehsan, Malaysia

⁎ Corresponding author.

Email address: edwardt@sunway.edu.my (E.R.T. Tiekink)

Received:

ABSTRACT

This bibliographic review summarises the coordination chemistry of mono- and di-selenium analogues of metal dithiocarbamate ligands, $[RR'NCS_2]^-$, as revealed by X-ray crystallography and spectroscopy (^{77}Se NMR and infrared). The Se-ligands are usually chelating but, bridging modes, up to μ_4, are known. Reflecting the larger size, greater polarisability and presence of a polar-cap (σ-hole), selenium atoms are more likely to be involved in secondary-bonding (chalcogen-bonding) than sulphur when a competition exists. Isostructural relationships are established across the series in about one-third of the structures.

Keywords: Selenothiocarbamate; Diselenocarbamate; Dithiocarbamate; Structures; Supramolecular chemistry; Secondary-bonding; ^{77}Se NMR

Contents

1. Introduction

Dithiocarbamate ligands, (I), comprise the most important member of the 1,1-dithiolate class of ligands and their metal complexes are ubiquitous in coordination chemistry. The significant contribution of up to 40% of canonical form (II) to its electronic structure make dithiocarbamate ligands very effective chelators for metal centres and thus, practically all accessible elements of the Periodic Table form compounds with the dithiocarbamate ligand. Besides fundamental chemistry, e.g. the ability of dithiocarbamate ligands to stabilise higher than usual oxidation states, traditionally metal dithiocarbamates were of interest for applications such as in the vulcanisation of rubber, in agriculture and as flotation agents in the mining industry. More current applications relate to the exploration of their roles in biology, such as pharmaceutical potential [1, 2], e.g. as anti-cancer and anti-microbial agents, radiopharmaceuticals [3] and in chelation therapy [4], as single-source precursors for the production of nanomaterials [5, 6] and even for the generation of coordination polymers [7]. Reflecting the above, the structural chemistry of dithiocarbamates has attracted considerable attention for a long time and has been reviewed periodically [8-11].

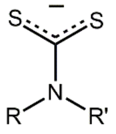
(I)

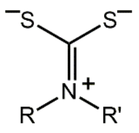
(II)

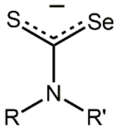
(III)

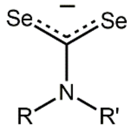
(IV)

R, R' = alkyl, aryl

In comparison to the very widely studied dithiocarbamates, the chemistry of selenium analogues, selenothiocarbamates (III) and diselenocarbamates (IV), is, relatively speaking, in its infancy. While dithiocarbamates are typically and readily prepared by reacting a secondary (sometimes primary) amine with CS_2 in the presence of base (usually alkali metal or ammonia), there are challenges associated with synthesising selenium analogues owing to the need to access C(S)Se and CSe_2, if an analogous procedure is to be followed to those employed for dithiocarbamates. When C(S)Se is available, the reaction to form selenothiocarbamates, with additional precaution, can be carried out as for the preparation of dithiocarbamates [12]. A second procedure, which may be more convenient, has been described very recently [13]. Here, in appropriate stoichiometric quantities, elemental sodium is reacted with selenium powder to generate Na_2Se, followed by reaction with $Me_2NC(=S)Cl$ to form $Na[Se(S=)CNMe_2]$. The diselenocarbamates are prepared in a similar fashion to that described for dithiocarbamates but, freshly prepared CSe_2 is recommended as are low temperatures and vigorous stirring [14]. The main motivation for synthesising selenium analogues of dithiocarbamates is to generate effective single-molecule precursors for potential semiconductor compounds as detailed below.

Over and above the consideration of molecular structures, secondary-bonding interactions important for supramolecular association have also been identified in the crystal structures described herein. Secondary-bonding interactions are well known and have been periodically reviewed [15-17], including in the context of metal dithiocarbamate chemistry for which it has been shown that steric effects can moderate supramolecular association mediated by M···S interactions leading to distinctive aggregation patterns [18-20]. Beyond structural chemistry, secondary-bonding involving chalcogens, while generally weak, are proven to be of importance in the design of materials and in catalysis [21]. Indeed, there has been renewed interest in recent years in secondary-bonding, mirroring the increasing interest in supramolecular chemistry in general, in fact so much so, that new terms have emerged for secondary-bonding depending on the Group the electrophilic atom belongs to, i.e. tetrel-, pnictogen- and chalcogen-bonding for elements of Groups 14, 15 and 16, respectively [22]. These efforts have led to an explanation of the seemingly curious observation often noted with secondary-bonding in that two ostensibly eletron-rich species are engaged in an attractive interaction. This phenomenon can be explained in terms of an anisotropic distribution of electron density leading to a so-called polar-cap or σ-hole concept [23-26]. In the context of the present discussion, for a covalent bond involving a chalcogen (Ch) atom, i.e. R–Ch, the outer lobe of the p-orbital forming this bond has an uneven distribution of electron-density with the region at the tip of the bonding vector being electron-deficient. This effect increases with increasing size of the element and so where competition between sulphur and selenium is possible, selenium would normally participate preferentially in secondary-bonding interactions.

This bibliographic review is arranged in the following manner: the significantly less numerous selenothiocarbamate structures are discussed before the diselenocarbamates. As a general principle, the structures of the oxidation products are described before salts, transition metal complexes and main group element compounds of the respective ligands. Within each category, the complexes/compounds are covered in order of groups of the Periodic Table. Within each group, the structures of lighter elements are described before heavier congeners, binary compounds before mixed ligand species, and neutral molecules before charged species. Data employed in this review were extracted in the form of Crystallographic Information Files (CIF's) with three-dimensional atomic coordinates archived from the Cambridge Structural Database [27] with structural interrogation largely dependent on PLATON [28]. All crystallographic diagrams are original, being drawn with DIAMOND [29]. Structures with disorder were omitted only in cases where the disorder led to ambiguous chemistry. In addition to structures determined by X-ray crystallography, information about structures revealed by ^{77}Se NMR spectroscopy and infrared spectroscopy are also included. The use of ^{77}Se NMR in research, a tool not usually available in the study of dithiocarbamates, was first reported in 1973 [30] and has enabled the determination of useful structural information in solution of organoselenium compounds in general, and selenothiocarbamates and diselenocarbamates in particular [31, 32].

2. Selenothiocarbamate structures

Two general approaches have been established for the synthesis of dialkylselenothiocarbamates. The first of these approaches is directly analogous to the common method used for the synthesis of the corresponding dithiocarbamates, namely the reaction of CSSe with the appropriate dialkylamine, yielding the dialkylammonium salt (Scheme 1).

$$2\ R_2NH + CSSe \rightarrow [R_2NH_2][R_2NC(S)Se]$$

Scheme 1

More recently, owing to the difficulty of obtaining CSSe, dialkylselenothiocarbamates have been prepared from Na_2Se, generated in situ by reaction of sodium and selenium powder, and the corresponding dialkylthiocarbamyl chloride (Scheme 2); see for example [13].

$$Na_2Se + R_2NC(S)Cl \rightarrow Na[R_2NC(S)Se] + NaCl$$

Scheme 2

2.1 Structures of oxidation products

The thiuramdiselenides, $[R_2NC(=S)Se]_2$ (**1-4**), are formed on oxidation of the corresponding selenothiocarbamates: oxidation occurs readily under mild conditions [14, 33, 34]. Thus, for example, **1**, was obtained on the attempted recrystallisation of $Me_2NCSSeNa$ from methanol [13]. Whereas the parent selenothiolates are only soluble in highly polar solvents, the thiruamdiselenides dissolve more readily, for example in dichloromethane or chloroform.

There are four X-ray structures conforming to the general formula [$R_2NC(=S)Se]_2$, **1-4** [13, 35, 36] with the R = Me (**1**) compound illustrated in Fig. 1. The non-hydrogen atoms in **1** lie on a crystallographic mirror plane and at the same time lie about a 2-fold axis of symmetry perpendicular to this plane, i.e. the molecule has 2/m symmetry. Key geometric parameters are listed in Table 1 and these provide reliable estimates for the values of formal C–Se and C=S bond lengths for selenothiocarbamates. From symmetry, the disposition of the thione-S atoms is anti. The molecular structures of the R = Et (**2**) [35] and i-Pr (**3**) [36] compounds follow the same trends, Table 1, but, each is disposed about a centre of inversion with the central N(S=)CSe–SeC(=S)N moiety being essentially planar. The exceptional structure is found when R = Cy (**4**) [35]. Here, there is no crystallographically imposed symmetry and the central N(S=)CSe–SeC(=S)N residue deviates greatly from planarity. Thus, while the C–Se–Se–C dihedral angle in each of **1**-**3** is 180° (from symmetry), the equivalent angle in **4** computes to 94.0(3)° indicating a + anti-clinal disposition of the N(S=)CSe groups.

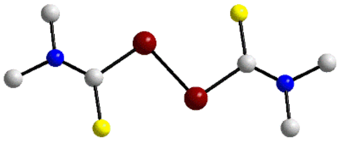

Fig. 1. The molecular structure of [$Me_2NC(=S)Se]_2$ (**1**) [13]. Colour code: brown, selenium; yellow, sulphur; blue, nitrogen; grey, carbon. Hydrogen atoms are omitted for reasons of clarity.

The formation of **1** agrees with suggestions that selenolates have a higher reactivity toward oxidation in comparison to thiolates. Compounds **2** and **4** [35] were obtained as oxidation products of selenothiocarbamate ions [$R_2NC(=)SSe]^-$ and their properties in solution were characterised by ^{77}Se NMR spectroscopy.

Measured ^{77}Se NMR data for **1**–**4** are reported in Table 2, along with those for all other selenothiocarbamate compounds discussed in section 2. The ^{77}Se chemical shifts for **1**-**4** span the range 798–860 ppm, relative to $\delta(Me_2Se) = 0$. The relatively high chemical shifts observed in these compounds, as compared to the other selenothiocarbamate and diselenocarbamate compounds reported herein, and other comparable examples [37], may be indicative of some charge delocalisation, leading to a partial positive charge on the selenium atom. This observation is consistent with the planarity of the NC(=S)Se–SeC(=S)N moiety noted in the X-ray structures.

Table 1

Geometric parameters (Å, °) for $[R_2NC(=S)Se]_2$

Compd	R	Se–Se	C_q–Se	C_q–S	Se–C–S	C–Se–Se	REFCODE	Ref.
1	Me	2.3576(8)	1.955(6)	1.676(6)	120.2(3)	93.33(18)	**SADQIA**	[13]
2	Et	2.3447(11)	1.952(5)	1.657(7)	120.5(4)	93.69(18)	**AJOZII**	[35]
3	iPr	2.3429(6)	1.952(3)	1.670(3)	119.26(16)	94.46(10)	**VETBUS**	[36]
4	Cy	2.3418(18)	1.967(8)	1.665(8)	119.1(4)	103.0(2)	**AJOZOO**	[35]
			1.926(8)	1.647(7)	119.2(2)	103.0(3)		

Table 2

^{77}Se NMR data (δ, ppm) for $[RR'NC(=S)Se]_2$

Compound	R, R'	^{77}Se (C=Se)[a]	Ref.
1	Me	na[b]	[13]
2	Et	835	[35]
3	i-Pr	na[b]	[36]
4	Cy	827	[35]
	Morpholine	801	[35]
	Pyrrolidyl	798	[35]
	Benzyl	860	[35]

a with reference to Me_2Se

b na = not available

Supramolecular association via Se···S chalcogen-bonding is found in each of **1** [13] and **2** [35]. The key feature of each supramolecular architecture is the formation of eight-membered {···SeSeCS}$_2$ synthons which are linked into a slightly kinked supramolecular tape as illustrated for **2** [35] in Fig. 2; in **1**, the tape is strictly planar. In **2**, the Se···S separation is 3.69 Å which is marginally less than the sum of the van der Waals radii for these atoms of 3.70 Å [38]. With smaller R = Me substituents, the molecules approach each other at closer distances, i.e. 3.51 Å in **1**. With larger R groups, the molecules do not form secondary-bonding interactions. Such interplay between the steric profile of R and secondary-bonding interactions is well documented in main group element dithiocarbamate structures [18-20].

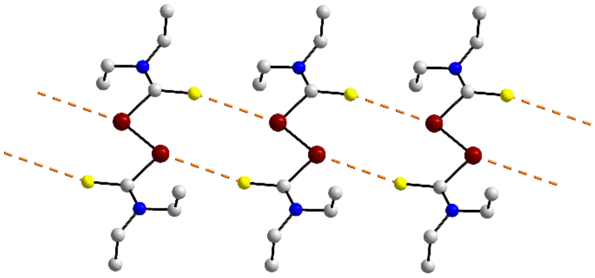

Fig. 2. The supramolecular tape in the crystal of [$Et_2NC(=S)Se]_2$ (**2**) [35] whereby eight-membered {···SeSeCS}$_2$ synthons are mediated by Se···S chalcogen bonds (3.69 Å).

2.2 *Alkali metal salt*

The chemistry of the alkali metal salts of carbamodichalcogenoates has received relatively scant attention. The pale-yellow sodium and potassium salts, M[$SeSCNMe_2$], may be synthesised in good yield (70-85%) from the reaction of the corresponding thiocarbamyl chloride with sodium or potassium selenide in acetonitrile (Scheme 2). The heavier metal congeners (M = Rb and Cs) are best prepared by treating the trimethylsilyl esters, $Me_2NC(S)SeSiMe_3$ with the appropriate metal fluoride [39].

Reaction of the salts with methyl iodide produces the corresponding Se–Me and S–Me derivatives, with the Se–Me derivative, $Me_2NC(S)SeMe$, predominant, the ratio is > 4:1; with more bulky alkyl halides, the ratio may exceed 9:1. Reaction with other Group 14 and 15 halides, such as $Ph_{4-x}MX_x$ (M = Si, Ge, Sn, Pd, P, As and Sb) gives the expected Se-metallated derivatives, $[MPh_{4-x}][Me_2NC(S)Se]_x$ [39].

There is a sole example of a selenothiocarbamate salt structure, namely $K_2[SeSCNMe_2].2CH_3CN$ (**5**) [39], which was prepared from the reaction of N,N-dimethylthiocarbamoyl chloride and potassium selenide in acetonitrile at 0°C under argon and was characterised by IR, ^1H, ^{13}C and ^{77}Se spectroscopies as well as by its subsequent conversion into methyl, phenacyl or 2-acetophenoneoxime esters [39]. The interest in the salt is not so much the actual structure per se, rather what can be learnt about the coordinating potential of the anion. The first point of note is that there is positional disorder in the selenium/sulphur atoms. There are two independent anions in the asymmetric unit and each displays disorder, one in the ratio 0.52:0.48 and the other less pronounced at 0.64:0.36. This observation points to the exchangeability of the donor atoms and thereby, indicates some equivalence in their coordinating ability. This equivalency is supported by the relatively high ^{77}Se NMR chemicals shifts observed in the salts (see below). As seen from Fig. 3(a), the selenothiocarbamate anion coordinates via both donor atoms with the nominal selenium atom bridging four potassium cations and the sulphur atoms linking two; the second independent anion coordinates in a similar fashion. For the least disordered anion, the range of K···Se distances of 3.32 to 3.42 Å exceeds that for the K···S separations of 3.30 to 3.31 Å. Globally, the structure comprises layers as shown in Fig. 3(b).

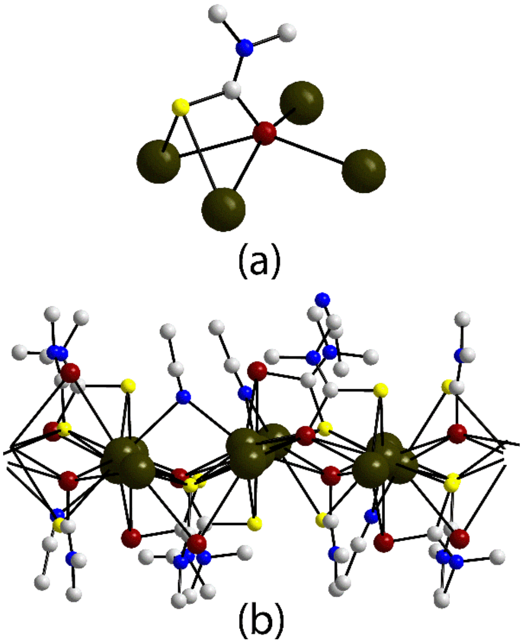

Fig. 3. (a) A view of the coordination mode for one of the independent anions in $K_2[SeSCNMe_2].2CH_3CN$ (**5**) [39], and (b) a view of the layer in the crystal. Additional colour code: potassium, olive-green.

Several ^{77}Se NMR data have been reported for a number of dialkyl selenothiocarbamate salts of Group I, namely $[R_2CN(=S)Se]M$, where R = Me or Et and M = Na, K, Rb or Cs, Table 3. The chemical shifts, approximately $\delta = 540+/-40$, are significantly greater than those observed in the corresponding selenocarbamate salts, $M[R_2NC(=O)Se]$ [37], perhaps indicative of greater π-delocalisation from selenium to sulphur than from selenium to oxygen, in accord with the greater π-basicity of sulphur. This observation is in keeping with there being little chemical distinction between sulphur and selenium in the selenothiocarbamates (see above).

Table 3

^{77}Se and ^{13}C NMR data (δ, ppm) for selected metal selenothiocarbamates[a]

Formula	^{77}Se (C=Se)[b]	^{13}C (C=Se)
$Na[Se(S)NCMe_2]$	503.2	207.3
$K[Se(S)NCMe_2]$ (5)	505.7	206.5
$Rb[Se(S)NCMe_2]$	575.7	206.8
$Cs[Se(S)NCMe_2]$	529.2	207.0
$Na[Se(S)NCEt_2]$	582.4	204.4
$K[Se(S)NCEt_2]$	583.8	204.7
$Me_2NC(S)SeMe$	486.4	195.2
$Me_2NC(Se)SMe$	539.7	200.5
$Me_2NC(S)SeGePh_3$	529.0	188.5
$Me_2NC(S)SeSnPh_3$	590.5	189.6
$Me_2NC(S)SeSnPh_2$	592.0	191.1
$Me_2NC(S)SePbPh_3$	633.9	191.3
$Me_2NC(S)SePPh_2$	655.7	191.5
$Me_2NC(S)SeAsPh_2$	670.4	191.5
$Me_2NC(S)SeAsPh$	624.8	193.1
$Me_2NC(S)SeSiMe_3$ (mixture)	na[c]	190.8, 192.9

a data for $Na[Se(S)NCMe_2]$ are from [13] and the rest are from [39]

b with reference to Me_2Se

c na = not available

2.3 Transition metal complexes

The homoleptic bis- and tris-(selenothiocarbamate) complexes $M[Se(S)CNR_2]_x$ (for x = 3, M = Ga, In, Tl, Cr, Fe, Co (**6**), Rh and Mn; for x = 2, M = Zn, Cd, Pb, Ni, Pd and Cu (**9**) and for x =1, M = Tl and Ag), for which compounds **6** [33] and **9** [40] have been structurally characterised, were prepared by reaction of the ammonium, sodium or potassium selenothiocarbamate salts with either the metal trichloride or the metal sulphate [12, 41, 42].

There are only four transition metal selenothiocarbamate complexes that have been structurally characterised by X-ray crystallography. The molecular structure of $Co(SeSCNEt_2)_3$ (**6**) [36] is shown in Fig. 4. The cobalt(III) centre is situated on a 2-fold axis of symmetry which bisects one of the selenothiocarbamate ligands, implying statistical disorder of the selenium and sulphur atoms for this ligand. Further, the ligand related across this axis is also disordered, in a ratio 0.65:0.35. Thus, as for **5** above, there is an indication of equivalent coordinating ability of the donors atoms in the selenothiocarbamates. In **6**, the cobalt(III) centre exists in a nominally S_3Se_3 donor set that defines a distorted octahedral geometry. The major reason for the distortion arises from the restricted bite distances of the selenothiocarbamate ligands which twists the octahedral faces towards a trigonal prismatic geometry. Despite the disorder, there is evidence for the Co–Se bond being longer than the Co–S bond for the symmetry-independent selenothiocarbamate ligand, i.e. 2.37 vs 2.34 Å; the Co–S/Se bond for the ligand bisected by the 2-fold axis is intermediate at 2.36 Å.

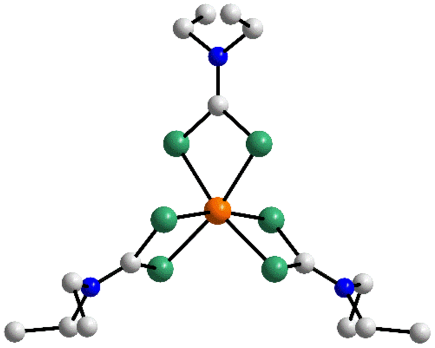

Fig. 4. The molecular structure of Co(SeSCNEt$_2$)$_3$ (**6**) [36]. Additional colour code: sea-green, hybrid selenium and sulphur, reflecting the partial occupancy of each site by these atoms.

The neutral square-planar complex, (Ph$_3$P)Ni(SeSCNMe$_2$)Br (**7**) [13], prepared from the 1:1 molar reaction of (PPh$_3$)$_2$NiBr$_2$ with sodium dimethylselenothiocarbamate, is shown in Fig. 5(a). This structure is unusual from a crystallographic point of view in that there are six independent molecules in the asymmetric unit. However, the six molecules are chemically similar. While some selenium/sulphur positional disorder in the structure is evident from a careful inspection of the anisotropic displacement parameters, it was concluded this was small and therefore, was not modelled [13]. The selenothiocarbamate ligand is chelating with the selenium atom occupying a position trans to the bromide atom. For the six independent molecules, the average Ni–Se bond length is 2.30 Å which is about 0.05 Å longer than the average Ni–S bond length of 2.25 Å. With a greater level of precision in the structure of **7**, a comment is possible on the relative lengths of the C–Se vs C–S bond lengths which are at least 0.11 Å longer in the former.

The homoleptic complexes mentioned above may undergo ligand exchange reactions, producing mixed ligand complexes, such as **8**, which forms on refluxing a 1:1 chloroform/acetonitrile solution of Ni[Se(S)CNEt$_2$]$_2$ and [NBu$_4$]$_2$[Ni(mnt)] (mnt = 1,2-dicyanoethene-1,2-dithiolate) [43]. Salt **8** is a relatively rare example of a nickel(II) complex with both S- and Se- ligands co-ordinated to the metal. The anion in [Bu$_4$N]{Ni(SeSCNEt$_2$)[S$_2$C$_2$(NC)$_2$]}.0.5MeC(=O)Me (**8**) [43], is shown in Fig. 5(b) and features a square-planar nickel(II) centre. As seen previously, there is positional disorder in the selenium/sulphur positions, with the ratio in this case being 0.67:0.33. Nevertheless, the Ni–Se bond length is greater than that of Ni–S, i.e. 2.33 cf. 2.28 Å; the Ni–S bonds formed by the di-negative dicyanoethene-1,2-dithiolate ligand are significantly shorter but, essentially the same at 2.14 and 2.15 Å with the bond trans to selenium being the shorter.

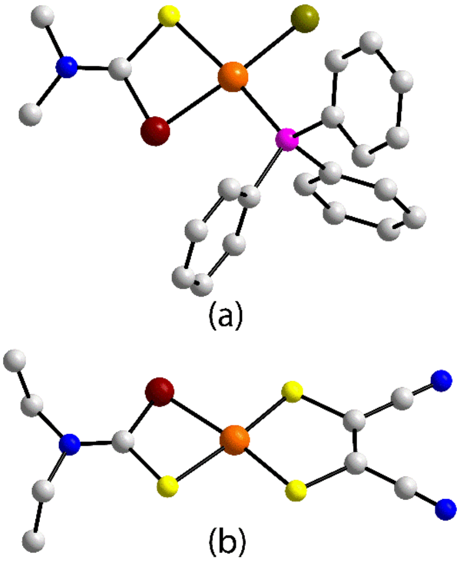

Fig. 5. The molecular structures of (a) $(Ph_3P)Ni(SeSCNMe_2)$ (**7**) [13] and (b) the anion in $[Bu_4N]\{Ni(SeSCNEt_2)[S_2C_2(NC)_2]\}.MeC(=O)Me$ (**8**) [43]. Additional colour code: pink, phosphorous; dark-yellow, bromide.

The fourth transition metal structure to be described in this section is a binary copper(II) complex, $Cu(SeSCNEt_2)_2$ (**9**) [40]. Here, the copper atom is chelated by two selenothiocarbamate ligands which define a square-planar geometry, within a trans-S_2Se_2 donor set. The Cu–Se bond lengths of 2.49 and 2.51 Å are systematically longer than the Cu–S bonds of 2.34 and 2.35 Å. In the crystal of **9**, centrosymmetric aggregates are formed via Cu···Se interactions of 2.89 Å so that the coordination of copper might be considered 4+1, Fig. 6.

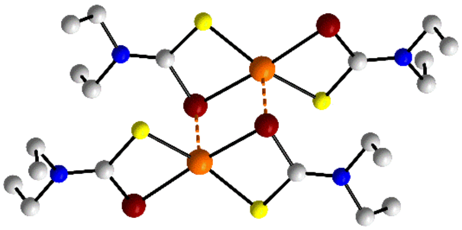

Fig. 6. Dimer formation via Cu···Se interactions (2.89 Å; orange dashed lines) in the crystal of $Cu(SeSCNEt_2)_2$ (**9**) [40].

2.4 *Main group element compounds*

There are two main group elements of selenothiocarbamate ligands available in the literature and these are two binary indium(III) structures, i.e. $In(SeSCNR_2)_3$ for R = Et (**10**) and i-Pr (**11**) [36]. These are isostructural with the cobalt(III) complex, $Co(SeSCNEt_2)_3$ (**6**) [36], Fig. 4, and present the same statistical disorder for the ligand about the 2-fold axis and fractional disorder for the second independent selenothiocarbamate ligand, i.e. with a Se:S ratio of 0.67:33 for **10** and 0.82:0.18 for **11**, indicating a mixture of isomeric structures.

Although the X-ray structures have not been reported, and perhaps to some extent falling outside the general scope of this review, a number of Group XIV and XV selenothiocarbamates have been synthesised and their NMR reported [39]. The NMR studies are noteworthy because of the paucity of ^{77}Se data for such compounds in the literature, and because at least one of the compounds displays dynamic behaviour which helps provide further insight on the structure and bonding. Key ^{13}C and ^{77}Se NMR data are collected in Table 3 (see above).

No ^{77}Se NMR signal was observed for the compound $Me_2NC(S)SeSiMe_3$ and at ambient temperature both the ^{1}H and ^{13}C spectra reveal exchange broadening, which disappears on cooling. At 258 K, two signals, in an approximate 1:1 ratio, are observed in the ^{1}H NMR spectrum at δ = 0.94 and 0.54 ppm, assignable to the hydrogen nuclei of the trimethylsilyl group, i.e. SSiC**H**$_3$ and SeSiC**H**$_3$, respectively. Correspondingly, the two ^{13}C signals at δ = 192.9 (>**C**=Se) and 190.8 (>**C**=S) ppm, assignable to the quaternary-carbon atom are observed in the ^{13}C NMR spectrum. These observations are consistent with the presence of two tautomeric forms, namely $Me_2NC(=S)Se–SiMe_3$ and $Me_2NC(=Se)S–SiMe_3$, which are in dynamic equilibrium [39]. This behaviour appears to be unique to these selenothiocarbamate compounds and lends support to the rational for the relatively high ^{77}Se chemicals shifts observed in $[R_2NC(S)Se]^-$ compounds, as already discussed.

3. Diselenocarbamate structures

3.1 Spectroscopic data

Characteristic IR spectral data for the complexes discussed in this section are collected in Table 4 [44-49]. The C–N stretching frequency lies in the range 1487–1511 cm^{-1}, bands indicative of partial double character in the C–N bond. The range is similar to that found for selenothiocarbamates but rather narrower than that found in the more studied dithiocarbamate complexes. This observation is presumably reflective of the paucity of data, rather than anything else. The C–Se stretch is found in the region 820–870 cm^{-1}, approximately 100 wavenumbers lower than that observed for corresponding C–S stretch in dithiocarbamate complexes, while the metal–Se stretch occurs in the region 311–503 cm^{-1}. There are insufficient examples to draw any inferences on the metal or coordination mode dependence of the M–Se stretching frequencies, but it is noteworthy that in the two lead(II) complexes for which data have been reported, the frequency is somewhat lower [311 (complex) and 349 cm^{-1}] than that found in the other complexes reported in Table 4. Available multinuclear magnetic resonance data are collated in Table 5 [44-52]. Individual results are discussed in the relevant sections below. Particularly noteworthy is the observation that the ^{13}C(C=Se) resonances are significantly upfield compared with their dithiocarbamate counterparts consistent with selenium being less electronegative than sulphur.

Table 4

IR data for selected metal diselenocarbamates

Compound	Formula	*v*(C–N)	*v*(C–Se)	*v*(Se–M)	Ref.
28	$[MeZnSe_2CNEt_2]_2$	1511	851	458	[44]
29	$[EtZnSe_2CNEt_2]_2$	1510	850	461	[44]
	$[MeCdSe_2CNEt_2]_2$	1504	821	469	[44]
30	$[neopentylZnSe_2CNEt_2]_2$	1499	854	457	[45]
	$[Me_3CZnSe_2CNEt_2]_2$	1504	853	466	[45]
32	$Zn(Se_2CNEt_2)_2(pyridine)$	1508	837	447	[46]
34	$[neopentylCdSe_2CNEt_2]_2$	1496	846	429	[47]
35	$[MeCdZnSe_2CNEt_2]_2$	1505	824, 850	458, 472	[44]
	$(2,4,6\text{-}Me_3C_6H_2Se)Zn(Se_2CNEt_2)]_2$	1503	850	472, 503	[46]
38	$Pb(Se_2CNEt_2)_2$	1485 (1495) [a]	843 (849) [a]	311 (310) [a]	[48]
	$Pb[Se_2CN(Me)Hex]_2$	1493	870	349	[48]
	$Bi(Se_2CNEt_2)_3$	1493	820	na[b]	[49]
39	$Bi[Se_2CN(n\text{-}Bu)_2]_3$	1487	851	na[b]	[49]

$Bi[Se_2CN(n\text{-}Bu)Me]_3$	1493	865	na[b]	[49]
$Bi[Se_2CN(Me)Cy]_3$	1496	857	na[b]	[49]

a Raman value in brackets

b na = not available

Table 5

^{77}Se and ^{13}C NMR data (δ, ppm) for selected metal diselenocarbamates

Compound	Formula	^{77}Se(C–Se)[a]	^{77}Se (C–Se–X)[a]	^{13}C(C–Se)	Ref.
23	$[Cu_4(\mu_4\text{-}H)Cu_4(Se_2CNEt_2)_6]PF_6$	364.8	na[b]	na[b]	[50]
	$[Cu_4(\mu_4\text{-}D)Cu_4(Se_2CNEt_2)_6]PF_6$	365.2	na[b]	na[b]	[50]
24	$\{Cu_4(\mu_4\text{-}H)Cu_4[Se_2CN(n\text{-}Pr)_2]_6\}PF_6$	374.9	na[b]	na[b]	[50]
	$\{Cu_4(\mu_4\text{-}D)Cu_4[Se_2CN(n\text{-}Pr)_2]_6\}PF_6$	376.9	na[b]	na[b]	[50]
25	$Cu_4(\mu_4\text{-}H)(\mu_3\text{-}Cu)_3(Se_2CNEt_2)_6$	443.8	na[b]	na[b]	[50]
	$Cu_4(\mu_4\text{-}D)(\mu_3\text{-}Cu)_3(Se_2CNEt_2)_6$	443.5	na[b]	na[b]	[50]
26	$Cu_4(\mu_4\text{-}H)(\mu_3\text{-}Cu)_3[Se_2CN(n\text{-}Pr)_2]_6$	448.6	na[b]	na[b]	[50]
	$Cu_4(\mu_4\text{-}D)(\mu_3\text{-}Cu)_3[Se_2CN(n\text{-}Pr)_2]_6$	449.7	na[b]	na[b]	[50]
28	$[MeZn(Se_2CNEt_2]_2$	na[b]	na[b]	188.3	[44]
29	$[EtZn(Se_2CNEt_2)]_2$	na[b]	na[b]	188.6	[44]
	$[MeCd(Se_2CNEt_2)]_2$	na[b]	na[b]	183.7	[44]
30	$[neopentylZn(Se_2CNEt_2)]_2$	na[b]	na[b]	188.3	[45]
	$[Me_3CZn(Se_2CNEt_2)]_2$	na[b]	na[b]	188.1	[45]

31	$\{Zn(Se_2CN(Me)(CH_2)_3NMe_2)_2\}_n$	666/642	na[b]	na[b]	[51]
	$\{Cd(Se_2CN(Me)(CH_2)_3NMe_2)_2\}_n$	736/708	na[b]	na[b]	[51]
	$(2,4,6\text{-}Me_3C_6H_2Se)Zn(Se_2CNEt_2)$	na[b]	na[b]	191.3	[46]
32	$Zn(Se_2CNEt_2)_2$(pyridine)	na[b]	na[b]	189.9	[46]
34	(neopentyl)$Cd(Se_2CNEt_2)$	na[b]	na[b]	182.2	[47]
35	$[MeCdZn(Se_2CNEt_2)_2]$	na[b]	na[b]	189.8	[44]
38	$Pb(Se_2CNEt_2)_2$	na[b]	na[b]	190.6	[48]
	$Pb[Se_2CN(Me)Hex]_2$	na[b]	na[b]	192.2	[48]
	$Bi(Se_2CNEt_2)_3$	na[b]	na[b]	192.0	[49]
39	$Bi[Se_2CN(n\text{-}Bu_2)]_3$	na[b]	na[b]	192.3	[49]
	$Bi[Se_2CN(n\text{-}Bu)Me]_3$	na[b]	na[b]	193.4	[49]
	$Bi[Se_2CN(Me)Cy]_3$	na[b]	na[b]	193.3	[49]
43	$PhSeC(=Se)NMe_2$	670.5	727.5	196.8	[52]
	$p\text{-}TolSeC(=Se)NMe_2$	663.5	716.9	197.4	[52]
	$(4\text{-}BrPh)SeC(=Se)NMe_2$	660.0	720.5	195.9	[52]
	$BzSeC(=Se)NMe_2$	606.6	644.5	196.2	[52]

Me$_2$NC(Se)SPh	607.5	na[b]	199.5	[52]
Me$_2$NC(Se)SBz	547.8	na[b]	198.3	[52]
Me$_2$NC(Se)Cl	715.5	na[b]	174.4	[52]

a with reference to Me$_2$Se

b not available

3.2 *Transition metal complexes*

The neutral homoleptic bis- and tris-(diselenocarbamate) complexes, $[M(Se_2CNR_2)_x]$ (x = 2 or 3) may be prepared from the metal trichloride or metal sulphate and the appropriate diselenocarbamate salt, using the same method as that described above for the selenothiocarbamate analogues. The cationic iron(IV) complexes, $[Fe(Se_2CNR_2)_3]^+$, are readily prepared as their tetrafluoroborate salts from the neutral iron(III) complexes, $[Fe(Se_2CNR_2)_3]$, by reaction with gaseous BF_3 in the presence of air, in exactly the same fashion as for the analogous dithiocarbamate complexes [53]. The ready accessibility of these complex cations are of particular interest because of the paucity (comparatively) of synthetic iron(IV) complexes known, despite their role in some biologically important systems, such as peroxidases and cytochrome c oxidase [54-56]. The availability of these iron(IV) complexes reveals the ability of the diselenocarbamate ligands to stabilise higher than usual oxidation states.

3.2.1 *Iron complex*

The sole example of an iron complex is found in the salt $[Fe(Se_2CNBenzyl_2)_3][BF_4]$ (**12**) [57], having an iron(IV) centre, an observation confirmed by supporting Mössbauer, X-ray photoelectron, electron spin resonance, magnetochemical and conductance measurements. As seen from Fig. 7, the iron atom is within a distorted octahedral geometry. The Fe–Se bond lengths lie in the narrow range 2.39 to 2.43 Å.

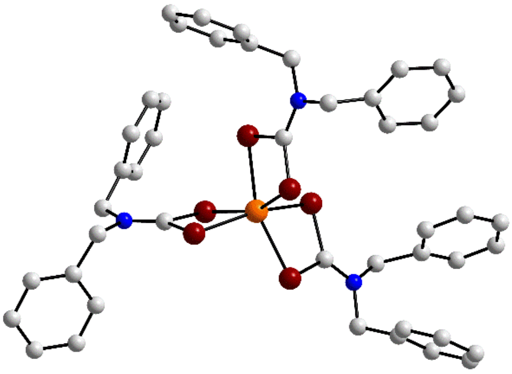

Fig. 7. The molecular structure of the cation in [Fe($Se_2CNBen_2)_3$][BF_4] (**12**) [57].

3.2.2 *Cobalt complex*

The structure of Co($Se_2CNEt_2)_3$ (**13**) [36] is isostructural with Co($SeSCNEt_2)_3$ (**6**) [36] shown in Fig. 4 but, obviously does not display analogous positional disorder. The Co–Se bond lengths in the octahedral complex lie in the narrow range 2.38 to 3.29 Å.

3.2.3 *Nickel group complexes*

The common features of M($Se_2CNR_2)_2$, M = Ni and R = Et (**14**) [58], M = Ni and R = n-Bu (**15**) [59]; M = Pd and R = i-Bu (**16**) [60], and M = Pt and R = i-Bu (**17**) [32], illustrated in Fig. 8, is the presence of a centre of inversion in the molecule, a symmetric mode of coordination of the diselenocarbamate ligand and a square-planar geometry about the metal centre. Key geometric parameters for **14-17** are collected in Table 7. The symmetric mode of coordination results in equivalent quaternary-C–Se bond lengths. Also noteworthy are the short quaternary-C–N bond lengths, an observation consistent with a significant contribution of the canonical structure with formal negative charges on each selenium atom and a positive charge on the nitrogen atom, i.e. $^{(2-)}Se_2C{=}N^{(+)}R_2$, to the overall electronic structure and equivalent to (II).

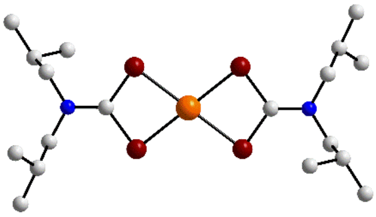

Fig. 8. The molecular structure of $Pt(Se_2CN\text{-}i\text{-}Bu_2)_2$ (**17**) [32].

Table 7

Geometric parameters (Å, °) for $M(Se_2CNR_2)_2$, M = Ni, Pd and Pt

Compd	M	R	M–Se	quaternary-C–Se	quaternary-C–N	REFCODE	Ref.
14	Ni	Et	2.4250(6), 2.4294(6)	1.8587(5), 1.8497(5)	1.299(2)	**NISECB10**	[58]
15	Ni	n-Bu	2.3067(12), 2.3169(12)	1.8517(9), 1.8683(9)	1.3404(7)	**BUSECN**	[59]
16	Pd	i-Bu	2.4292(15), 2.4376(11)	1.888(7), 1.876(7)	1.310(8)	**JAMJAI**	[60]
17	Pt	i-Bu	2.4250(6), 2.4294(6)	1.8587(5), 1.8497(5)	1.3829(4)	**SECBPT**	[32]

Each of **14-16** feature close Se···Se contacts in their respective crystals but, only in **14** [58] are these less than the sum of two times the van der Waals radii of selenium, i.e. 3.80 Å [38]. While the cut-off based on the sum of van der Waals radii is convenient, it does not imply no secondary-bonding interaction exists between the selenium atoms in **15** and **16** [61, 62]. As seen from Fig. 9, Se···Se contacts, i.e. 3.709(6) Å, link molecules of **14** into a linear supramolecular chain.

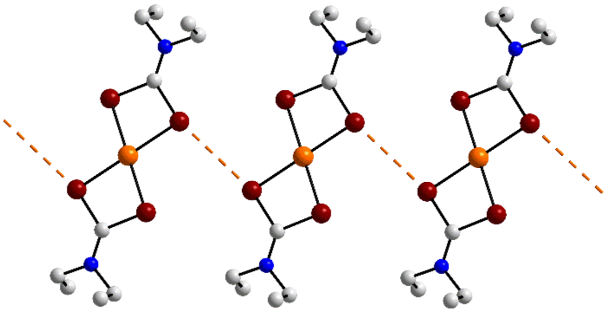

Fig. 9. The linear supramolecular chain mediated by Se···Se chalcogen-bonding (3.71 Å) in the crystal of $Ni(Se_2CNEt_2)_2$ (**14**) [58].

The relatively great ability of the diselenocarbamate ligands to stabilise higher than usual oxidation states is further demonstrated by the stability of complex **18**, which was prepared by the oxidation of $[Ni(Se_2CN^{n}Bu_2)_2]$ by Br_2 [63]. The nickel(IV) cation in $\{Ni[Se_2CN(n\text{-}Bu)_2]_3\}Br$ (**18**) [64] is located on a crystallographic site of symmetry $\bar{3}$ with the independent Ni–Se bond length being 2·391(5) Å. The structure is closely related to **12** [57], Fig. 7, but, has higher symmetry although it is noted there is considerable disorder in the n-butyl chains. The structures of **12** [57] and **18** [64] indicate the diselenocarbamate ligand is capable of stabilising higher than usually observed oxidation states.

The homoleptic compounds mentioned above may serve as precursors to mixed ligand complexes, through ligand exchange. Thus, for example, **19** and **20** are produced on mixing equimolar amounts of [n-$Bu_4N]_2$[ML] and [M($Se_2CNEt_2)_2$] (M = Ni, L = $S_2C_2(NC)_2$; M = Pd, L = $Se_2C_2S_2C$=S) [65, 66], while [Pt(Se_2CNR_2)PR'$_3$Cl] (R, R' = alkyl or aryl) may be prepared from [Pt($Se_2CNR_2)_2$] and [Pt($PR'_3)_2Cl_2$]. Subsequent halide exchange gives access to the heavier halogen congeners [32]. The next two structures to be described are mixed ligand salts with a chelating 1,2-dithiolate ligand in **19**, i.e. [n-Bu_4N]{Ni(Se_2CNEt_2)[$S_2C_2(NC)_2$]} [65], and a 1,2-diselenolate ligand in **20**, i.e. [n-Bu_4N][Pd(Se_2CNEt_2)($Se_2C_2S_2C$=S)] [66]. The molecular structure of the anion in **19** resembles that shown in Fig. 5(b) for square-planar {Ni(SeSCNEt$_2$)[$S_2C_2(NC)_2$]}$^-$ in **8** [43] but, with two Ni–Se bond lengths of 2.31 and 2.37 Å cf. the Ni–Se and Ni–S bond lengths of 2.15 and 2.08 Å. The square-planar anion in **20** is illustrated in Fig. 10 and features two equivalent Pd–Se bond lengths of 2 x 2.44 Å for the diselenocarbamate ligand which are a little longer than the two Pd–Se bond lengths of 2 x 2.41 Å formed by the dinegative ligand.

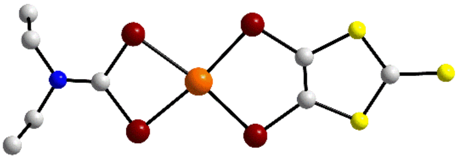

Fig. 10. The molecular structure of the anion in [n-Bu_4N][Pd(Se_2CNEt_2)($Se_2C_2S_2C$=S)] (**20**) [66].

3.2.4 Copper complexes

To a first approximation, the binary copper(II) complex Cu($Se_2CNEt_2)_2$ (**21**) [58, 67], resembles that described above for **9** [40], Fig. 6. However, the coordination geometry is significantly distorted from ideal square-planar as seen in the dihedral angle of 21° between the two chelate rings. The range of Cu–Se bond lengths for the non-symmetric molecule is 2.41 to 2.45 Å with the longest of these associated with the selenium atom forming an intermolecular Cu···Se interaction of 2.91 Å with a centrosymmetrically-related molecule, Fig.

11 so, again as for **9** [40], the coordination might be described as being 4 + 1. The remaining structures to be discussed contain copper(I) and are polynuclear.

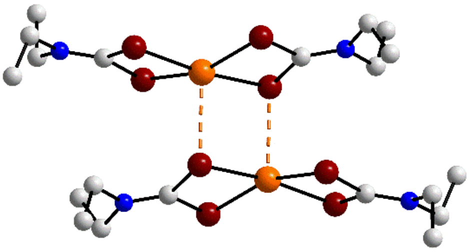

Fig. 11. The dimeric aggregate in $Cu(Se_2CNEt_2)_2$ (**21**) [67] mediated by Cu$\cdots$Se secondary-interactions (2.91 Å; orange dashed lines).

Motivated by the desire to synthesise molecules for evaluation as single-source precursors for copper selenide nanomaterials, a series of copper(I) diselenocarbamate clusters were prepared [50]. The copper(I) cluster $[Cu_4(Se_2CNn\text{-}Pr_2)_4]$ (**22**) was prepared by reaction of $[Cu(NCMe)_4][PF_6]$ and $[n\text{-}Pr_2NH_2][Se_2CNn\text{-}Pr_2]$ in THF. Clusters (**23**) and (**24**) were prepared from (**22**) or its ethyl analogue, $[Cu_4(Se_2CNEt_2)_4]$, by addition of $LiAlH_4$. Further reduction of (**23**) and (**24**) with $LiAlH_4$ yields (**25**) and (**26**). Reduction with $NaBD_4$ in place of $LiAlH_4$ gives the deuterated analogues. These are the first examples of copper(I) clusters supported by diselenocarbamates [50].

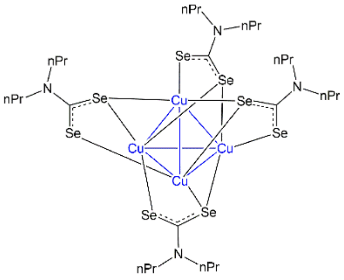

22

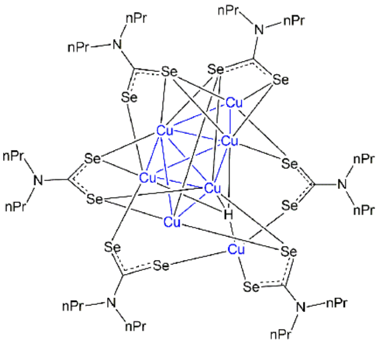

24

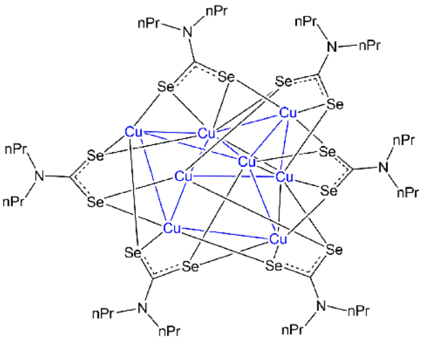

26

The X-ray crystal structures are available for the air- and moisture-sensitive copper(I) clusters **22-26**. The smallest of these, $[Cu_4Se_2CNn\text{-}Pr_2]_4$ (**22**), is tetranuclear, 2-fold symmetric and features a tetrahedron of copper(I) atoms with Cu···Cu edges, Fig. 12(a). While each diselenocarbamate ligand coordinates in essentially the same manner, capping a tetrahedral face by bridging two copper atoms via a single selenium atom, and being connected to the third copper atom via the second selenium atom, two of the edges are not bridged by a singly-bridging selenium atom. This has the consequence that the edge lengths for the latter, at 2.77 and 2.81 Å, are longer than the remaining four edges, i.e. 2.63 to 2.65 Å. Octanuclear complexes of composition $[Cu_4(\mu_4\text{-}H)Cu_4(Se_2CNEt_2)_6]PF_6$.acetone (**23**) and n-propyl analogue $\{Cu_4(\mu_4\text{-}H)Cu_4(Se_2CNn\text{-}Pr_2)_6\}PF_6$ (**24**) were also structurally characterised in the study [50]. The cation in **24** is shown in Fig. 12(b). Despite the presence of significant disorder in the structure and complexity of the image, the 3-fold symmetric molecule is relatively easy to describe. The four central copper atoms describe a tetrahedron with independent Cu···Cu distances of 2.84 and 2.96 Å. Each tetrahedral face is capped by a copper atom with Cu···Cu distances being shorter than for the central tetrahedron being in the range 2.58 to 2.67 Å. The μ_4-hydride atom is located within the central tetrahedron. The Cu_8H atoms are encapsulated by 12 selenium atoms each of which is biconnective; taken by themselves, the selenium atoms define an icosahedron. The ethyl analogue **23** resembles closely that just described but, the cation has 2-fold symmetry. Reduction of each of **23** and **24** yields heptanuclear clusters $Cu_4(\mu_4\text{-}H)(\mu_3\text{-}Cu)_3(Se_2CNEt_2)_6$ (**25**) and $Cu_4(\mu_4\text{-}H)(\mu_3\text{-}Cu)_3(Se_2CNn\text{-}Pr_2)_6$ (**26**) [50]. The relationship between the two pairs of structures is quite straightforward in that one of the capping copper(I) atoms of **23** and **24** is no longer present in **25** and **26**. The central Cu_4 core is tetrahedral, the μ_4-hydride atom occupies an interstitial site, and the remaining three copper atoms each cap a tetrahedral face so the 3-fold symmetric core is tricapped tetrahedral as illustrated for **26** in Fig. 12(c). Two distinct coordination modes are found for the diselenocarbamate ligands, one being triconnective as in **22** and the other being tetraconnective as in each of **23** and **24**. Again, the shell defined by the 12 selenium atoms defines an icosahedron. Finally, and consistent with the chemical reduction, the two sets of Cu···Cu separations are reduced to 2.86 to 2.92 Å within the tetrahedron and 2.48 to 2.58 Å for the capping interactions. Overall, the X-ray structures of these complexes were supported by the multinuclear ^{1}H, ^{2}H, ^{31}P and ^{77}Se NMR spectroscopic studies, photophysical data as well as ESI mass spectrometry. Of interest was that ^{77}Se NMR indicated the clusters were fluxional in solution.

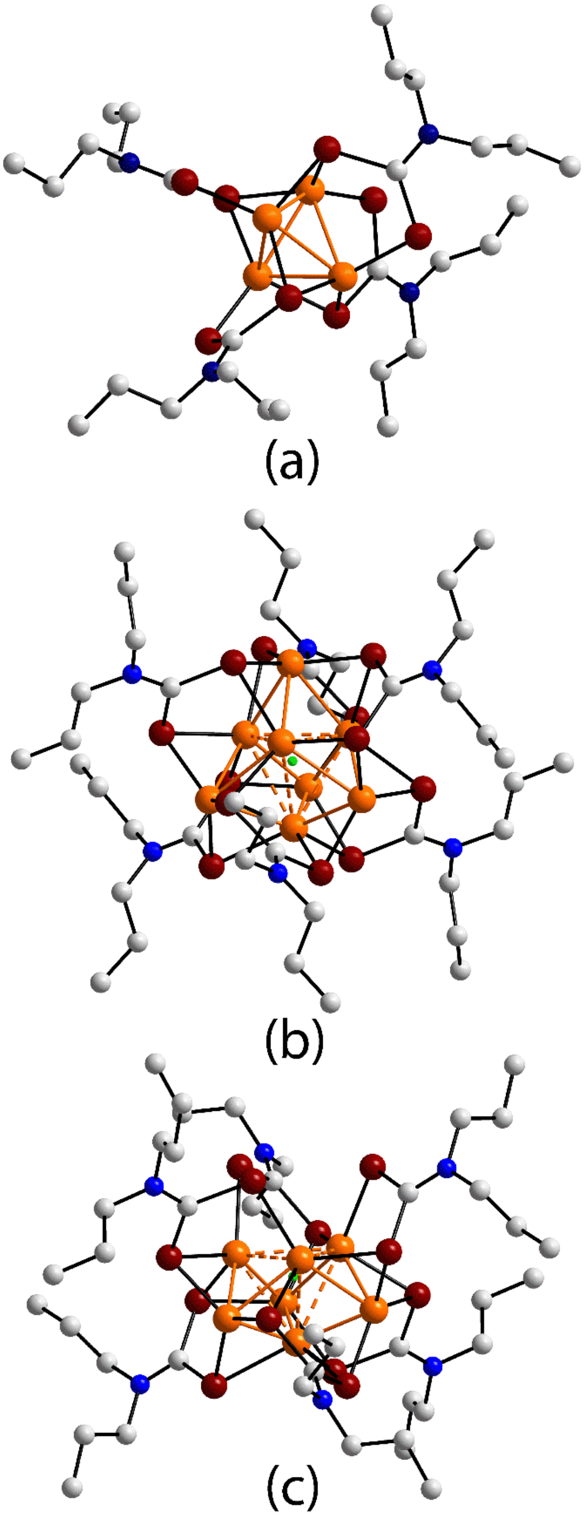

Fig. 12. Molecular structures of (a) $[Cu_4Se_2CNn\text{-}Pr_2]_4$ (**22**) [50], (b) $\{Cu_4(\mu_4\text{-}H)Cu_4(Se_2CNn\text{-}Pr_2)_6\}^+$ (**24**) [50] and (c) $Cu_4(\mu_4\text{-}H)(\mu_3\text{-}Cu_3)_3(Se_2CNn\text{-}Pr_2)_6$ (**26**) [50]. In (b) and (c), the central Cu_4 tetrahedron is highlighted with orange dashed lines, and the hydride is shown as a green sphere.

3.3 Main group element compounds

Like their transition metal counterparts, many homoleptic diselenocarbamate complexes of the main group elements may be readily synthesised from the metal halides, sulphates or nitrates and the corresponding diselenocarbamate salts. Thus, for example, $[Zn(Se_2CNEt_2)_2]_2$ (**27**) [58], $[Zn(Se_2CN(Me)CH_2CH_2NMe_2]_n$ (**31**) [51], $[In(Se_2CNEt_2)_3]$ (**36**) [68] and $[Pb(Se_2CNEt_2)_2]$ (**38**) [48] may be prepared by the simple addition of dialkyldiselenocarbamate to a solution of the metal salt [44, 48, 51, 68]. The alkyl-zinc and -cadmium compounds $[RM(Se_2CNR'_2)]$, **28-30** [44, 45] and **33** [69], which are of interest because of their potential as single-source precursors for zinc selenide and cadmium selenide, are accessible in high yield via comproportionation of the homoleptic selenocarbamates with either dialkylzinc or dialkylcadmium compounds. An alternative method is the insertion of CSe_2 into the M–N bond of the corresponding alkylmetal amides, $RM–NR'_2$ [44, 45, 69]. Comproportionation of $[Cd(Se_2CNEt_2)_2]$ with $ZnMe_2$ gives the mixed Zn/Cd compound, (**35**) [44].

3.3.1 Zinc structures

There are several examples of zinc compounds of diselenocarbamates with most investigations being motivated by the quest to synthesise zinc selenide nanomaterials. This quest was due to the on-going interest in obtaining potential single-molecule precursors for the deposition by metal-organic chemical vapour deposition (MOCVD) of binary and ternary materials, such as zinc selenide, as these are important II/VI semiconductors. The structure of $\{Zn(Se_2CNEt_2)_2\}_2$ (**27**) [58] is a centrosymmetric dimer with equal numbers of chelating and bidentate bridging ligands, Fig. 13(a). From the geometric data collected in Table 8, there is a measure of asymmetry in the Zn–Se bonds formed by the chelating ligand but, not for the bridging ligand. A transannular Zn···Se interaction of 3.03 Å is noted that gives rise to a 4+1 coordination geometry which is highly distorted. Overall, the molecule has a step-ladder topology. The binuclear structures for **27** [58] and cadmium(II) analogue **33** [69] (see below) conform to the common structural motif found for molecules of the general formula $[M(S_2CNR_2)_2]_2$ except when the steric bulk of R precludes close approach of the molecules so that a mononuclear tetrahedral motif is observed instead [18].

There are three organozinc compounds whereby two diselenocarbamate ligands have been replaced by organic substituents, i.e. Me (**28**), Et (**29**) [44] and neopentyl (**30**) [45]. Each molecule is located about a centre of inversion; there are two independent half molecules in the asymmetric unit of **30**. As seen from Fig. 13(b), each diselenocarbamate ligand is chelating while simultaneously bridging the centrosymmetrically-related zinc atom. As highlighted in Table 8, the selenium atom involved in the bridge forms systematically longer Zn–Se bond lengths with the bridging Zn–Se bond length being the longer bond in each case. As for **27**, overall, each molecule has a step-topology.

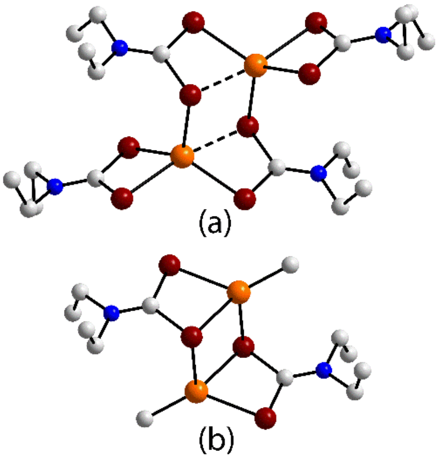

Fig. 13. Molecular structures of (a) $\{Zn(Se_2CNEt_2)_2\}_2$ (**27**) [58] and (b) $[MeZn(Se_2CNEt_2)]_2$ (**28**) [44]. In (a), the dashed lines indicate transannular Zn···S interactions.

Table 8

Geometric parameters (Å, °) for M(Se_2CNEt_2)$_2$ and RM(Se_2CNEt_2)

Compd	M	R	M–Se(chelating)	M–Se(bridging)	M–Se(transannular)	REFCODE	Ref.
27	Zn	–	2.4462(16), 2.5684(19)	2.4353(13), 2.492(3)	3.033(2)	**ESECZN**	[58]
28	Zn	Me	2.4814(15), 2.5864(18)	2.6343(18)	–	**JOYCAB**	[44]
29	Zn	Et	2.484(6), 2.590(6)	2.617(6)	–	**JOYCAB**	[44]
30	Zn	neopentyl	2.475(3), 2.589(3)	2.656(3)	–	**JUGMON**	[45]
			2.486(3), 2.577(3)	2.630(2)			
33	Cd	–	2.7137(18), 2.646(2)	2.6344(16), 2.725(2)	2.9549(16)	**JOWRES**	[69]
34	Cd	neopentyl	2.645(3), 2.807(3)	2.813(4)		**WEKMOO**	[47]
35	Zn/Cd	Me	2.5747(16), 2.6815(18)	2.7422(18)		**JOYCAB**	[44]

In $\{Zn(Se_2CN(Me)(CH_2)_3NMe_2)_2\}_n$ (**31**) [51], the diselenocarbamate ligands carry additional functionality capable of coordinating zinc. One of the ligands does in fact form a Zn–N bond leading to a one-dimensional coordination polymer as shown in Fig. 14. The diselenocarbamate ligands are chelating but, with significant differences in the Zn–Se bond lengths, i.e. 2.452(2) and 2.774(3) Å, and 2.4346(18) and 2.778(3) Å. The NSe_4 coordination geometry is based on a square-pyramid with the amine-nitrogen atom in an apical position. The topology of the supramolecular chain is zig-zag.

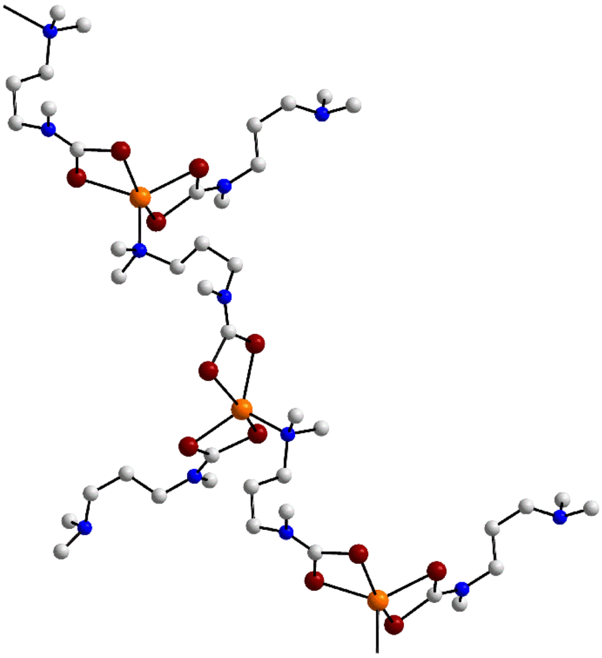

Fig. 14. The one-dimensional coordination polymer in the crystal of $\{Zn(Se_2CN(Me)(CH_2)_3NMe_2)_2\}_n$ (**31**) [51].

The final zinc structure is closely related to that just described for **31** [51]. In mononuclear $Zn(Se_2CNEt_2)_2$(pyridine) (**32**) [46], Fig. 15, although there is reduced asymmetry in the Zn–Se bond lengths, i.e. 2.475(3) and 2650(2) Å, and 2.482(2) and 2.696(2) Å. As with **31** [51], to a first approximation the NSe_4 donor set is based on a square-pyramid.

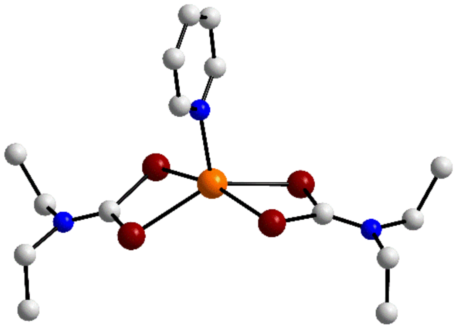

Fig. 15. The molecular structure of Zn(Se_2CNEt_2)$_2$(pyridine) (**32**) [46].

3.3.2 Cadmium structures

There are two cadmium diselenocarbamate structures in the literature, namely Cd(Se_2CNEt_2)$_2$ (**33**) [44] and RCd(Se_2CNEt_2) for R = neopentyl (**34**) [47]. The third structure with cadmium also contains zinc whereby the cadmium and zinc atoms are statistically disordered, i.e. R = Me (**35**) [69]. The molecular structures and trends in key geometric parameters, Table 8, follow those described above for their lighter congeners. Reflecting the larger size of the cadmium atom, the transannular Cd···Se distance is comparatively shorter than the equivalent separation in the zinc analogue, Table 8. It is noted that one of the independent molecules in **34** [47] is badly disordered and so data for this molecule are not included in Table 3. The bond lengths exhibited in disordered **35** [69], which is isostructural with the all-zinc compound **28** [44], have intermediate values reflecting the disorder.

The hydrogen atoms of the metal-methyl group in the mixed metal, dimeric complex [$Me_2CdZn(Se_2CNEt_2)$] display a single signal at -17.20 ppm in the ^{77}Se NMR (ambient temperature) [44], Table 5. The M-methyl group in the analogous zinc complex, [MeZn(Se_2CNEt_2)]$_2$, resonates at significantly higher frequency, namely $\delta = -9.42$ ppm, similar to the Zn-methyl shift in the analogous dithiocarbamate compounds [70]. The observation of a single M–C**H**$_3$ signal, and the significant difference in the chemical shifts, have been interpreted as arising from exchange of methyl groups between cadmium and zinc. Analogous methyl group exchange between zinc and cadmium is well known in mixtures of the dimethyl compounds $CdMe_2$ and $ZnMe_2$ [71].

3.3.3 *Indium structures*

The two known octahedral indium(III) structures, $In(Se_2CNR_2)_3$ for R = Et (**36**) [68], Fig. 16, and i-Pr (**37**) [36] conform to those found for the monoselenothiocarbamates described in 2.4 and by implication to $Co(SeSCNEt_2)_3$ (**6**) [36] illustrated in Fig. 4.

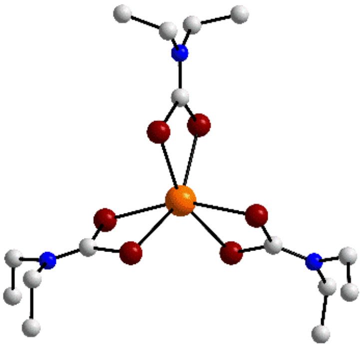

Fig. 16. The molecular structure of $In(Se_2CNEt_2)_3$ (**36**) [68].

3.3.4 *Lead(II) structure*

There is a sole example of a lead(II) structure, $Pb(Se_2CNEt_2)_3$ (**38**) [48], which is another example of a metal compound synthesised to be investigated as single-molecule precursor to produce lead selenide (PbSe) nanocrystals by thermolysis in tri-n-octylphosphine oxide. Here, both diselenocarbamate ligands chelate the lead(II) centre with one ligand coordinating a little more asymmetrically, i.e. Pb–Se = 2.849(3) and 3.103(3) Å, than the other, i.e. Pb–S = 2.827(4) and 2.952(3) Å. Taking into account the projected position of the stereochemically-active lone-pair of electrons, the $(lp)S_4$ donor set defines a distorted trigonal-bipyramidal geometry with the less tightly bound selenium atoms in axial positions (140°). Secondary- (tetrel-) bonding with Pb···Se separations of 3.47 and 3.62 Å lead to a supramolecular chain with a zig-zag topology, Fig. 17. An alternate description of the coordination geometry taking into account the additional interactions would be a capped octahedral geometry with the lone-pair projecting out through the trigonal face defined by the selenium atoms forming the longer Pb···Se separation of the three pairs of bonds.

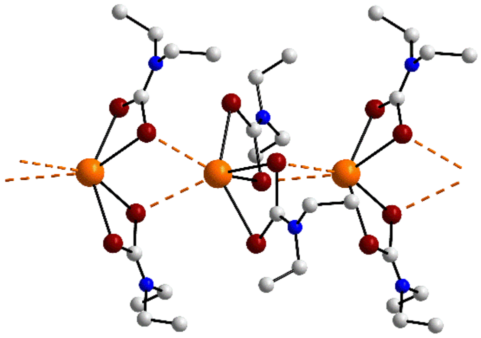

Fig. 17. Supramolecular zig-zag chain mediated by Pb···Se seconding-bonding interactions (3.47 and 3.62 Å) in the crystal of $Pb(Se_2CNEt_2)_2$ (**38**) [48].

3.3.5 Bismuth structure

The single example of a Group XV structure with a diselenocarbamate ligand is that of $Bi[Se_2CN(n-Bu)_2]_3$ (**39**) [49]. This compound was prepared in a single-pot synthesis by the addition of carbondiselenide to a methanolic solution of di-n-butylamine in the presence of Be_2O_3 [49]. The motivation behind its synthesis was, as with many of the other homoleptic compounds, to explore its potential utility as a single-source precursor for the deposition of bismuth selenide films on glass substrates through aerosol-assisted metal-organic chemical vapour deposition (AA-MOCVD). Bismuth selenide is known to be a narrow band gap semiconductor of interest for solid-state thermoelectric devices such as in the use for cooling and for power-generating devices operating near room temperature [49]. There are two independent molecules in the asymmetric unit but, these do not significantly differ from each other. The bismuth centre is chelated by three ligands which exhibit different levels of asymmetry in their mode of coordination with a range of Bi–Se bond lengths of 2.8440(13) to

3.1084(10) Å for the first independent molecule and a slightly wider range of 2.8058(10) to 3.0837(10) Å for the second molecule. Centrosymmetrically-related molecules approach each other at the faces defined by the longer Bi–Se bonds formed by each ligand to form Bi···Se secondary interactions and dimeric aggregates, Fig. 18. The Bi···Se separations are 3.39 and 3.49 Å for the independent dimers.

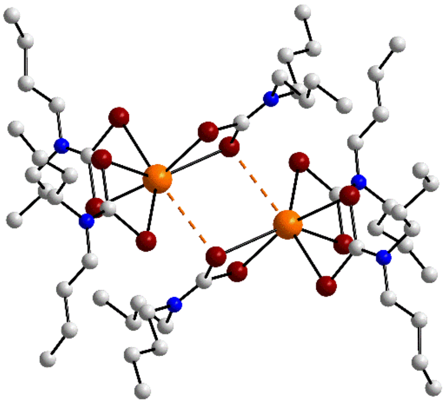

Fig. 18. Supramolecular dimer mediated by Bi···Se seconding-bonding interactions (3.49 Å) in the crystal of Bi[$Se_2CN(n\text{-}Bu)_2]_3$ (**39**) [49].

3.3.6 *Selenium structures*

The (dialkylselenothiocarbamoyl)diselenides readily disproportionate to yield the corresponding mono- and tri-selenides, $R_2NC(=Se)SeC(=Se)CNR_2$ and $Se(Se_2CNR_2)_2$, respectively. Thus **40**, for example, is obtained along with $Et_2NC(=Se)SeC(=Se)CNEt_2$ on aerial oxidation of (diethylselenothiocarbamoyl)diselenide [72]. Alternatively, **42** may be obtained via the reaction of bis(morpholinoselenocarbonyl)triselenide with iodide [73].

There are two binary selenium(II) structures, $Se(Se_2CNEt_2)_3$ (**40**) [72, 74] and $Se(Se_2CN(CH_2)_4)_3$ (**41**) [75]; the structure of the former has been determined twice and data from the most recent determination is used here. Compound **40** [72] was obtained from an attempt to prepare bis(N,N-diethylselenocarbamoyl)diselenide, which is a useful starting material in the preparation of derivatives of N,N-dialkyldiselenocarbamic acids, and was also obtained from the disproportion of sodium N,N-diethyl-1,1-diselenocarbamate [74]. In **40**, the central selenium(II) atom is coordinated by two asymmetrically coordinating, coplanar diselenocarbamate ligands with the two shorter Se–Se bonds [2.4501(11) and 2.4847(11) Å] lying to one side and the two longer Se–Se bonds [2.7981(12) and 2.8601(12) Å] to the other. The two lone-pairs of electrons are projected to lie over the weaker Se–Se bonds so that the $Se_4(lp)_2$ donor set is based on a skewed-trapezoidal bipyramidal geometry. In the crystal, the coordinating selenium atoms are associated via Se···Se chalcogen interactions of 3.69 and 3.76 Å with the result that a linear supramolecular chain is formed, Fig. 19. The molecular structures of the two independent molecules comprising the asymmetric unit of **41** are very similar to that in **40** but, each has 2-fold symmetry [75]. Each independent molecule self-associates into a linear supramolecular chain via Se···Se chalcogen interactions of 2 x 2.59 Å (from symmetry).

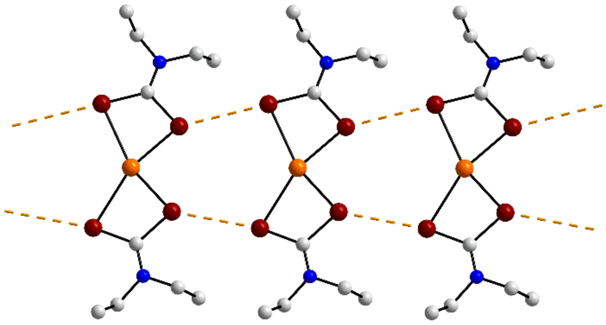

Fig. 19. Supramolecular zig-zag chain mediated by Se···Se seconding-bonding interactions (3.69 and 3.76 Å) in the crystal of $Se(Se_2CNEt_2)_3$ (**40**) [74]. To distinguish between the different selenium atoms in the structures, the central selenium atoms are shown as orange spheres in this and in Figs 20 and 21.

Skew-trapezoidal bipyramidal geometries are also found for each of the two independent molecules in the crystal of $Se[Se_2CN(CH_2CH_2)_2O]I$ (**42**) [73]. Crystals of **42** were obtained from the prolonged-standing of a very dilute solution from the reaction of bis(morpholinoselenocarbonyl)triselenide with iodine in a 1:1 ratio [73]. The short edge of the skew-trapezoidal plane comprises an symmetrically coordinating diselenocarbamate ligand [Se–Se = 2.36 and 2.38 Å for the first molecule, and 2.39 and 2.44 Å for the second] while the long edge is defined by the symmetrically bridging iodido atoms [Se–I = 3.15 and 3.18 Å for the first molecule, and 2 x 3.08 Å for the second]. The result of the bridging is a zig-zag chain as shown in Fig. 20.

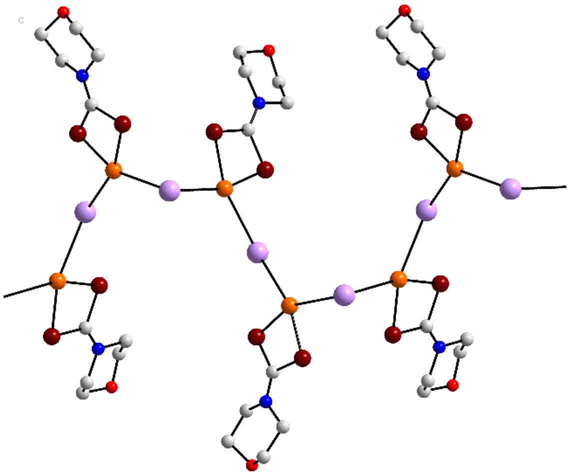

Fig. 20. Zig-zag chain in the crystal of Se[$Se_2CN(CH_2CH_2)_2O$]I (**42**) [73]. Extra colour code: iodide, lavender.

The final structure to be described is an organoselenium ester, PhSeC(=Se)NMe_2 (**43**), included here for the sake of completeness, which was obtained from the reaction of dichloromethylenedimethyliminium chloride with LiAlHSeH in anhydrous THF solution at 0 °C followed by the addition of a solution of PhSeLi under an argon atmosphere [52]. There is a significant disparity in the quaternary-C–Se and quaternary-C=Se bond lengths, i.e. 1.94 and 1.82 Å, as would be anticipated for an ester of this type. Chalcogen-bonding is found between the singly- and doubly-bonded selenium atoms in the crystal (3.71 Å) which leads to a helical chain, Fig. 21. The incoming selenide-Se atom is opposite to the quaternary-carbon atom (168°) and the resulting C_2Se donor atoms define a T-shaped geometry with the lone-pairs of electrons projected to lie over the vacant space opposite to the ipso-carbon atom.

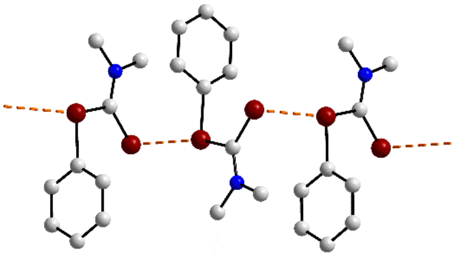

Fig. 21. Helical chain mediated by Se···Se seconding-bonding interactions (3.71Å) in the crystal of $PhSe(Se_2CNMe_2)$ (**43**) [52].

4 Relationship to dithiocarbamate structures

This section presents a discussion on the isostructural relationships existing between the structurally characterised selenothiocarbamates and diselenocarbamates, described above, and their dithiocarbamate analogues. The comparison is made on the basis of unit cell parameters in the absence of morphological data on individual crystals. While there are no all-selenium analogues of **1**-**4**, tetraalkylthiuram disulphide analogues are known for each of these [76-79], with interest in these systems owing in part to the medicinal applications of the ethyl derivative, known as Antabuse®, which inhibits the enzyme acetaldehyde dehydrogenase [80]. The common feature of the thiuram derivatives is the orthogonal relationship between the two halves of each molecule in stark contrast to the planar/near planar confirmations seen in **1**-**3**, but more akin to the twisted confirmation observed in **4**.

The generally symmetric tris(ligand) structures of cobalt(III), **6** and **13**, and those of indium(III), **10**, **11**, **36** and **37**, form an interesting series of compounds that has attracted considerable attention in terms of the adopted symmetry in the solid-state [36]. The common feature of the cobalt(III) structures with R = Et is that they crystallise in the C2/c space group and are isostructural with the dithiocarbamate analogue [81]; the molecules are 2-fold symmetric. The same space group and molecular symmetry is found for the indium(III) structures with R = i-Pr, **11** and **37**, and the dithiocarbamate analogue [82]. The indium(III) R = Et, structures comprise a more disparate series with **10** and the dithiocarbamate analogue [83] adopting the A2/a space group again with the molecules having 2-fold symmetry. The diselenocarbamate structure, **36**, is the outlier in that it crystallises in $P2_1/c$ space group with no crystallographically-imposed symmetry. The important consequence of the high symmetry imposed on the selenothiocarbamate structures is the disorder in their positions, as noted above.

Mixed ligand nickel(II) complexes with selenothiocarbamate **8** and diselenocarbamate **16** are isostructural but, there is no dithiocarbamate analogue. For the binary copper(II) complexes, the three diethyl analogues **9**, **21** and $Cu(S_2CNEt_2)_2$ [84] are isostructural. An isostructural relationship also exists for the nickel(II) analogues, i.e. **14** and $Ni(S_2CNEt_2)_2$ [85]. It is a noted that a tetragonal polymorph [86] also exists for $Ni(S_2CNEt_2)_2$ which differs in terms of the absence of C–H···π(chelate ring) interactions [87] which are present in the former. Diselenocarbamate **15** and its dithiocarbamate analogue [88] are also isostructural. An isostructural relationship exists between the iso-butyl diselenocarbamates of palladium(II) (**16**) and platinum(II) (**17**) but, these are not isostructural with the palladium(II) iso-butyl dithiocarbamate [89]. The tris(diselenocarbamate) anion of nickel(II), **18**, is isostructural with the dithiocarbamate analogues [90].

There are also several isostructural relationships among the compounds of the zinc-triad elements. The centrosymmetric binuclear molecules in isostructural **27** and **33** are isostructural with their dithiocarbamate analogues [91, 92]. Referring to Table 8, there are five organozinc/cadmium diselenocarbamate structures, with methyl derivatives **28** and mixed metal **35** being isostructural. Two organozinc dithiocarbamates have been structurally characterised and while the methylzinc dithiocarbamate [70] is not isostructural with **28** (or **35**), ethylzinc derivative **29** and the dithiocarbamate [93] analogue are. There are two polymorphs of the dithiocarbamate analogue of **32**. While one of these is isostructural [94], the other is not, having spontaneously resolved during crystallisation [95].

There is an isostructural relationship between the lead(II) compound **38** and the dithiocarbamate analogue although a space group ambiguity exists, i.e. Cc [96] versus C2/c [97] with the structure of **38** likely to conform to the higher symmetry. By contrast, the bismuth(III) structure is not isostructural with the dithiocarbamate analogue [98].

The remaining structures for which isostructural relationships potentially exist are the selenium compounds **40-43**. Of these, only the binary selenium(II) compound **40** has a direct equivalent in the literature, i.e. the non-isostructural analogue in the literature [99].

Although not mentioned in the original publication [50], there is a dithiocarbamate analogue (not isostructural) [100] to the Cu_4 diselenocarbamate cluster **22**. Non-isostructural analogues for the Cu_8 clusters **23** and **24** are also known [101].

Conclusions and outlook

Structural studies reveal that mono- and bi-selenium analogues of dithiocarbamate ligands are likely to chelate the central element with some instances of bridging, i.e. μ_2, μ_3 and up to μ_4-, being apparent, especially among copper(I) clusters and main group element compounds. Isostructural relationships exist across the selenothio-, diseleno- and dithio-carbamate series and when not isostructural, similar structures are often apparent. Chalcogen-bonding involving the selenium atom is sometimes observed in the crystal. From the foregoing, there are many gaps in knowledge of these systems and therefore, considerable scope for further work. Especially, as the utility of these compounds as single-source precursors for metal sulphide/selenide nanomaterials has been proven. Given the wide pharmacopeia of selenium compounds [102, 103], a strong case can also be made for exploring the biological potential of these selenium derivatives. In short, additional research in this class of compound is warranted in order to expand their use in materials science and to explore opportunities for developing new drugs.

Acknowledgements

We thank Sunway University for support of biological and crystal engineering studies of metal dithiocarbamates.

References

[1] G. Hogarth, Mini-Rev. Med. Chem. 12 (2012) 1202.

[2] V. Bala, G. Gupta, V.L Sharma, Mini-Rev. Med. Chem. 14 (2014) 1021.

[3] D.J. Berry, R.T.M. de Rosales, P. Charoenphun, P.J. Blower, Mini-Rev. Med. Chem. 12 (2012) 1174.

[4] M. Blanusa, V.M. Varnai, M. Piasek, K. Kostial, Curr. Med. Chem. 12 (2005) 2771.

[5] M.A. Malik, M. Afzaal, P. O'Brien, Chem. Rev. 110 (2010) 4417.

[6] C.E. Knapp, C.J. Carmalt, Chem. Soc. Rev. 45 (2016) 1036.

[7] E.J. Mensforth, M.R. Hill, S.R. Batten, Inorg. Chem. Acta 403 (2013) 9.

[8] D. Coucouvanis, Prog. Inorg. Chem. 26 (1979) 301.

[9] R.P. Burns, F.P. McCullough, C.A. McAuliffe, Adv. Inorg. Chem. 23 (1980) 211.

[10] G. Hogarth, Prog. Inorg. Chem. 53 (2005) 71.

[11] P.J. Heard, Prog. Inorg. Chem. 53 (2005) 1.

[12] R. Heber, R. Kirmse, E. Hoyer, Z. Anorg, Allg. Chem. 393 (1972) 159.

[13] M. El-khateeb, H. Görls, W. Weigand, L.R. Almazahreh, Polyhedron 106 (2016) 27.

[14] D. Barnard, D. T. Woodbridge, J. Chem. Soc. (1961) 2922.

[15] N.W. Alcock, Adv. Inorg. Chem. Radiochem. 15 (1972) 1.

[16] H.-B. Burgi, J. Dunitz, J. Am. Chem. Soc. 109 (1987) 2924.

[17] I. Haiduc, in J. L. Atwood, J. W. Steed, (Eds), Encyclopedia of Supramolecular Chemistry, vol. 2, Marcel Dekker Inc., New York (2004) p. 1215.

[18] E.R.T. Tiekink, CrystEngComm. 5 (2003) 101.

[19] E.R.T. Tiekink, CrystEngComm. 8 (2006) 104.

[20] E.R.T. Tiekink, J. Zukerman-Schpector, Coord. Chem. Rev. 254 (2010) 46.

[21] K.T. Mahmudov, M.N. Kopylovich, M.F.C Guedes da Silva, A.J.L. Pombeiro, Dalton Trans. 46 (2017) 10121.

[22] A.C. Legon, Phys. Chem. Chem. Phys. 19 (2017) 14884.

[23] P. Politzer, J.S. Murray and M.C. Concha, J. Molec. Model. 13 (2007) 643.

[24] A. Bauza, T.J. Mooibroek, A. Frontera, ChemPhysChem 16 (2015) 2496.

[25] M.H. Kolář, P. Hobza, Chem. Rev. 116 (2016) 5155.

[26] S. Scheiner, J. Phys. Chem. A 121 (2017) 5561.

[27] C.R. Groom, I.J. Bruno, M.P. Lightfoot, S.C. Ward, Acta Crystallogr., Sect. B: Struct. Sci. 72 (2016) 171.

[28] A.L. Spek, J. Appl. Crystallogr. 36 (2003) 7.

[29] K. Brandenburg, DIAMOND. Visual Crystal Structure Information System, version 3.1, Crystal Impact, Bonn, Germany, 2006.

[30] S. Gronowitz, I. Johnson, A. B. Hornfeldt, Chem. Scr. 3 (1973) 94.

[31] W.-H. Pan, J.P. Fackler Jr, J. Am. Chem. Soc. 100 (1978) 5783.

[32] W.-H. Pan, J.P. Fackler Jr, H.-W.Chen, Inorg. Chem. 20 (1981) 856.

[33] I. Ymén, Acta Chem. Scand. 37B (1983) 707.

[34] J. Finster, R. Heber, E. Hoyer, W.I. Nefedov, J.W. Salyn, Z. Chem. 14 (1974) 25.

[35] W. Dietzsch, J. Sieler, W. Meiler, W. Robien, Phosphorus Sulfur 38 (1998) 293.

[36] W. Dietzsch, N.V. Duffy, A.M. Lee, B.W. Skelton, A.H. White, Z. Anorg. Allg. Chem. 632 (2006) 2419.

[37] H. Duddeck, Ann. Rep. Ann. Rep. NMR Spect. 52 (2004) 105.

[38] A. Bondi, J. Phys. Chem. 68 (1964) 441.

[39] K. Kawai, K. Ibi, M. Ebihara, S. Kato, Z. Anorg. Allg. Chem. 633 (2007) 625.

[40] J. Kaiser, R. Richter, J. Sieler, Acta Crystallogr., Sect. B: Struct. Sci. 31 (1975) 2600.

[41] C. Furlani, E. Cervone, F.D. Camassei, Inorg. Chem. 7 (1968) 265.

[42] W. Dietzsch, D.L. Boyd, D.L. Uhrich, N.V. Duffy, Inorg. Chim. Acta 121 (1986) 19.

[43] H.J.B. Slot, R.C. Haltiwanger, V. Parthasarathi, M. Kolenbrander, P.T. Beurskens, W. Dietzsch, R. Kirmse, J. Crystallogr. Spectrosc. Res. 16 (1986) 617.

[44] M.B. Hursthouse, M.A. Malik, M. Motevalli, P. O'Brien, J. Mater. Chem. 2 (1992) 949.

[45] M.A. Malik, M. Motevalli, J.R. Walsh, P. O'Brien, Organometallics 11 (1992) 3136.

[46] M.A. Malik, M. Motevalli, P. O'Brien, Polyhedron 18 (1999) 1259.

[47] I. Abrahams, A. Malik, M. Motevalli, P. O'Brien, J. Organomet. Chem. 465 (1994) 73.

[48] T. Trindade, O.C. Monteiro, P. O'Brien, M. Motevalli, Polyhedron 18 (1999) 1171.

[49] O.C. Monteiro, T. Trindade, F.A.A. Paz, J. Klinowski, J. Waters, P. O'Brien, J. Mater. Chem. 13 (2003) 3006.

[50] R.S. Dhayal, J-H. Liao, H-N. Hou, R. Ervilita, P-K. Liao, C.W. Liu, Dalton Trans. 44 (2015) 5898.

[51] P. O'Brien, J.R. Walsh, I.M. Watson, M. Motevalli, L. Henriksen, J. Chem. Soc., Dalton Trans. (1996) 2491.

[52] M. Koketsu, Y. Fukuta, H. Ishihara, J. Org. Chem. 67 (2002) 1008.

[53] E.A. Pasek, D.K. Straub, Inorg. Chem. 11 (1972) 259.

[54] T.H. Moss, A. Ehrenberg A.J. Bearden, Biochemistry 8 (1969) 4159.

[55] R.H. Felton, G.S. Owen, D. Dolphin, J. Fajer, J. Am. Chem. Soc. 1 (1971) 6332.

[56] M. Wikström Proc. Natl. Acad. Sci. USA, 78 (1981) 4051.

[57] P. Deplano, E.F. Trogu, F. Bigoli, E. Leporati, M.A. Pellinghelli, D.L. Perry, R.J. Saxton, L.J. Wilson, J. Chem. Soc., Dalton Trans. (1983) pp. 25.

[58] M. Bonamico, G. Dessy, J. Chem. Soc. A (1971) 264.

[59] J.H. Noordik, J.M.M. Smits, Cryst. Struct. Commun. 3 (1974) 253.

[60] J.-C. Wang, J.P. Fackler Jr, Acta Crystallogr., Sect. C: Cryst. Struct. Commun. 45 (1989) 951.

[61] A. Mukherjee, G.R. Desiraju, IUCrJ 1 (2014) 49.

[62] Y.S. Tan, S.N. Abdul Halim, K.C. Molloy, A.L. Sudlow, A. Otero-de-la-Roza, E.R.T. Tiekink, CrystEngComm 18 (2016) 1105.

[63] H. C. Brinkhoff, J. A. Cras, J.J. Steggerda, J. Willemse, Rec. Trav. Chim. 88 (1969) 633.

[64] P.T. Beurskens, J.A. Cras, J. Cryst. Mol. Struct. 1 (1971) 63.

[65] J. Stach, R. Kirmse, U. Abram, W. Dietzsch, J.H. Noordik, K. Spee, K.P. Keijzers, Polyhedron 3 (1984) 433.

[66] R.-M. Olk, W. Dietzsch, J. Kahlmeier, P. Jörchel, R. Kirmse, J. Sieler, Inorg. Chim. Acta 254 (1997) 375.

[67] M. Bao, J. Weng, W. Su, R. Cao, M. Hong, Acta Crystallogr., Sect. C: Cryst. Struct. Commun. 56 (2000) e185.

[68] S. Saluschke, M. Pink, W. Dietzsch, R. Kirmse, Z. Anorg. Allg. Chem. 619 (1993) 1862.

[69] M.B. Hursthouse, M.A. Malik, M. Motevalli, P. O'Brien, Polyhedron 11 (1992) 45.

[70] M.B. Hursthouse, M.A. Malik, M. Motevalli, P. O'Brien, Organometallics 10 (1991) 730.

[71] I. Guijarro, in Z. Rappoport, I. Marek (Eds), Chemistry of Organozinc Compounds, Part I, John Wiley & Sons, Chichester (2006), p. 193.

[72] R.O. Gould, C.L. Jones, W.J. Savage, T.A. Stephenson, J. Chem. Soc., Dalton Trans. (1976) pp. 908.

[73] F. Bigoli, E. Leporati, M.A. Pellinghelli, G. Crisponi, P. Deplano, E.F. Trogu, J. Chem. Soc., Dalton Trans. (1983) pp. 1763.

[74] M. Bao, M. Hong, W. Su, R. Cao, Acta Crystallogr. Sect. C: Cryst. Struct. Commun. 56 (2000) e219.

[75] S. Esperås, S. Husebye, Å. Rolandsen, Acta Chem. Scand. A 29 (1975) 608.

[76] Y. Wang, J.H. Liao, Acta Crystallogr., Sect. B: Struct. Sci. 45 (1989) 65.

[77] I.L. Karle, J. A. Estlin, K. Britts, Acta Crystallogr. 22 (1967) 273.

[78] F. Jian, L. Jiang, H.-K. Fun, K. Chinnakali, I.A. Razak, X. You, Acta Crystallogr., Sect. C: Cryst. Struct. Commun. 55 (1999) 573.

[79] V.J. Hall, E.R.T. Tiekink, Z. Kristallogr. 210 (1995) 701.

[80] J. Mutschler, M. Grosshans, M. Soyka, S. Rösner, Pharmacopsychiatry 49 (2016) 137.

[81] P.C. Healy, J.W. Connor, B.W. Skelton, A.H. White, Aust. J. Chem. 43 (1990) 1083.

[82] S. Bhattacharya, N. Seth, V.D. Gupta, H. Noth, M. Thomann, Z. Naturforsch., B: Chem. Sci. 49 (1994) 193.

[83] K. Dymock, G.J. Palenik, J. Slezak, C.L. Raston, A.H. White, J. Chem. Soc., Dalton Trans. (1976) pp. 28.

[84] M. Bonamico, G. Dessy, A. Mugnoli, A. Vaciago, L. Zambonelli, Acta Crystallogr. 19 (1965) 886.

[85] M. Bonamico, G. Dessy, C. Mariani, A. Vaciago, L. Zambonelli, Acta Crystallogr. 19 (1965) 619.

[86] M.N.I. Khan, J.P. Fackler Jr, H.H. Murray, D.D. Heinrich, C. Campana, Acta Crystallogr., Sect. C: Cryst. Struct. Commun. 43 (1987) 1917.

[87] E.R.T. Tiekink, J. Zukerman-Schpector, Chem. Commun. 47 (2011) 6623.

[88] J. Lokaj, V. Vrábel, E.Kellö, Chem. Zvesti 38 (1984) 313.

[89] M.-L. Riekkola, T. Pakkanen, L. Niinistö, Acta Chem. Scand. A 37 (1983) 807.

[90] J.P. Fackler Jr, A. Avdeef, R.G. Fischer Jr, J. Am. Chem. Soc. 95 (1973) 774.

[91] M. Bonamico, G. Mazzone, A. Vaciago, L. Zambonelli, Acta Crystallogr. 19 (1965) 898.

[92] A. Domenicano, L. Torelli, A. Vaciago, L.Zambonelli, J. Chem. Soc.A (1968) pp. 1351.

[93] M.A. Malik, P. O'Brien, M. Motevalli, Acta Crystallogr., Sect. C: Cryst. Struct. Commun. 52 (1996) 1931.

[94] M.A. Malik, M. Motevalli, P. O'Brien, Polyhedron 18 (1999) 1259.

[95] A.V. Ivanov, V.I. Mitrofanova, M. Kritikos, O.N. Antzutkin, Polyhedron 18 (1999) 2069.

[96] H. Iwasaki, H. Hagihara, Acta Crystallogr., Sect.B: Struct. Crystallogr. Cryst. Chem. 28 (1972) 507.

[97] Z.V. Zvonkova, A.N. Khvatkina, N.S. Ivanova, Kristallografiya 12 (1967) 1065.

[98] R.-Z. Sun, Y.-C. Guo, W.-M. Liu, S.-Y. Chen, Y.-Q. Feng, Chin. J. Struct. Chem. 31 (2012) 655.

[99] A. Pollnitz, R.A. Varga, A. Silvestru, Acta Crystallogr., Sect. E: Struct. Rep. Online 67 (2011) o411.

[100] D. Cardell, G. Hogarth, S. Faulkner, Inorg. Chim. Acta 359 (2006) 1321.

[101] P.-K. Liao, C.-S. Fang, A.J. Edwards, S. Kahlal, J.-Y. Saillard, C.-W. Liu, Inorg. Chem. 51 (2012) 6577.

[102] E.R.T. Tiekink, Dalton Trans. 41 (2012) 6390.

[103] H.-L. Seng, E.R.T. Tiekink. Appl. Organomet. Chem. 26 (2012) 655.